ME 461:
Finite Element Analysis

Spring | 2016

The Development and Analysis of a Car Suspension System

Group Members:

Justin Rongier, Sarah Mistele, Hector Castro, Harshil Patel

PennState
College of Engineering

Department of Mechanical and Nuclear Engineering, University Park, PA

Table of Contents

Table of Contents 2
Executive Summary 3
Acknowledgements 4
Section 1: Background and Project Plan 7
Section 2: Development and Description of the CAD Geometry 8
Section 3: Development of Finite Element Meshes 10
Section 4: Development and Description of the Model Assembly and Boundary Conditions ..19
Section 5: Development and Description of Model Interactions 17
Section 6: Analysis of Finite Element Model 18
Section 7: Summary of Major Findings 20
Section 8: Works Cited 21
Appendix 1: Insert Title Here 2213

Executive Summary

A car's suspension system is responsible for reducing the displacement of the car body in response to disturbances in the surface of the road. Most shock absorbers use a combination of a spring, which converts the kinetic energy of the displacement into potential energy, and a viscous damper, which dissipates the energy. A series of mechanical linkages are responsible for transmitting the load from the road surface to the shock absorber, and the overall result of the system is that for any given base displacement, the car body will experience smaller and exponentially decaying perturbations.

In order to model this system, geometry for a shock absorber was located on GrabCAD and imported into Abaqus. This geometry was then simplified in order to reduce computational time; threading along the outside of the pressure tube was eliminated as it did not carry stress, and external details were minimized on bushings and the piston. Material properties were assigned per the literature, with the spring made of chrome vanadium, the bushings made of 1040 steel, and the pressure tube made of 6061 T6 Aluminum. For the loads on this system, a sinusoidal base displacement was applied while the top was held in place and the entire part was constrained for vertical motion only.

The resultant stresses in the system were maximum on the interior contact surface of the spring and at the neck of the top bushing. The magnitudes of these stresses were, as expected, highest at the highest base displacements. In this model the base displacements were higher than realistic values in order to show trends, so the stresses greatly exceed the material yield properties. Future iterations of this project would use more realistic displacements and loads in order to determine what parts need design considerations.

Acknowledgements

We would like to acknowledge and thank Dr. Kraft for his guidance throughout this project.

List of Figures

Section 1
1. Figure 1.1: Double Wishbone Car Suspension System……..Page 7

Section 2
2. Figure 2.1: Isometric View of Shock Absorber……..…Page 8
3. Figure 2.2: Dimensioned Drawing of Shock Absorber - units in m……...…Page 8

Section 3
4. Figure 3.1.1: Coil Spring Mesh…...……..……Page 10
5. Figure 3.1.2: View 1 of Coil Spring……...……...……Page 10
6. Figure 3.1.3: View 2 of Coil Spring……...……...……Page 10
7. Figure 3.1.4: View 3 of Coil Spring……..…Page 11
8. Figure 3.1.5: Density……..……...……Page 11
9. Figure 3.1.6: Young's Modulus and Poisson's Ratio……...…Page 11
10. Figure 3.2.1: Nut Mesh View 1…...……..…Page 12
11. Figure 3.2.2: Nut Mesh View 2……...……..…Page 12
12. Figure 3.3.1: Oil Piston……..……....……Page 12
13. Figure 3.3.2: Oil Piston……..……....……Page 12
14. Figure 3.3.3:View 1 of Oil Piston……..…..Page 13
15. Figure 3.3.4: View 2 of Oil Piston……....…..…..Page 13
16. Figure 3.3.5: View 3 of Oil Piston……Page 13
17. Figure 3.3.6: Density of Oil Piston……...…Page 14
18. Figure 3.3.7:Young Modulus and Poissons Ratio……..……..…Page 14
19. Figure 3.4.1: Washer……..……....…Page 14
20. Figure 3.4.2: View 1 of Washer……..……...……..…Page 15
21. Figure 3.4.3:View 2 of Washer……..……...……..…Page 15
22. Figure 3.4.4:View 3 of Washer..……..……...…Page 15
23. Figure 3.4.5:Density of Washer……..……...……..…Page 15
24. Figure 3.4.6: Youngs Modulus and Poissons Ratio……..……..…Page 15
25. Figure 3.5.1: Isometric View……..……...……..…Page 16
26. Figure 3.5.2: Cross Sectional View 1……..……..…Page 16
27. Figure 3.5.3: Cross Sectional View 2……..……..…Page 16
28. Figure 3.6.1: Isometric View……...……..……..…Page 17
29. Figure 3.6.2: Cross-Sectional View 1..……..……..…Page 17
30. Figure 3.6.3: Cross-Sectional View 2…...……..……..…Page 17
31. Figure 3.7.1: Pressure Tube…….Page 18
32. Figure 3.7.2: Pressure Tube View 2……Page 18
33. Figure 3.7.3: Pressure Tube top and bottom views…….Page 18

Section 1: Background and Project Plan

Objective: The goal of this project is to use the FEM to accurately model a car suspension system under oscillating loading conditions. We plan to analyze the structural integrity of the shock absorber and to visualize stress distributions to determine where we should design against part failure.

Background Information: A car suspension system is intended to dampen the vibration of a car's wheel in response to a disturbance in the road. This smooths out the ride of a car. Car suspensions do this by receiving a load and dissipating it into a damper. Dampers in vehicles are generally known today as shock absorbers. The force transmission through a car suspension is done by a series of mechanical links which eventually lead to a shock absorber. In general, shock absorbers have to be designed to be versatile. They must be able to dampen forces at high and low speeds, temperatures, and varying car weights. The complex system of mechanical links and required versatility of shock absorbers make car suspensions particularly interesting to analyze. The full mechanism is shown in the figures below, and includes springs, dampers, bushings, and linkages.

General Approach: The first step to our general approach will be to determine the complexity of the problem and to identify ways to simplify it. Once that is completed, we will identify the forces being applied to the suspension system, including those from the car mass and road roughness. We will attempt to geometrically model the entire system using available information, including all connecting parts. We will then develop a mesh for the system, using a finer mesh on curved parts or edges and a coarser mesh throughout rigid links. Material properties and functions for surface roughness will also be applied. We will follow the suspension assembly shown below.

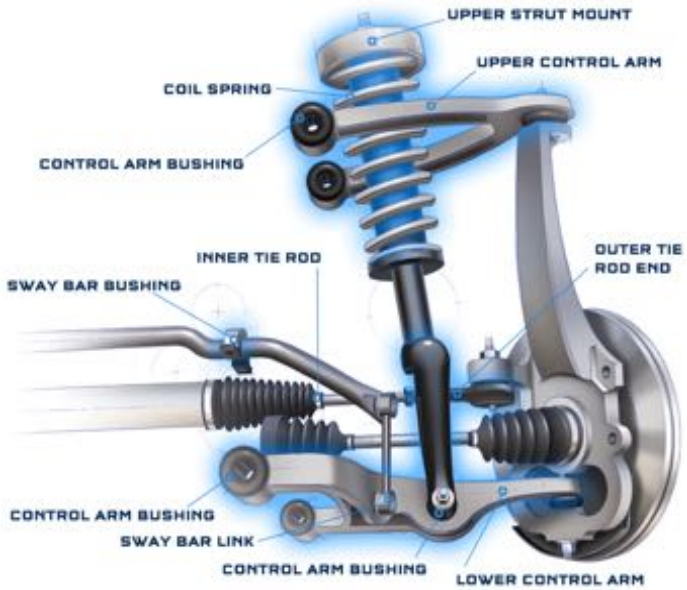

Figure 1.1: Double Wishbone Car Suspension

Section 2: Development and Description of the CAD Geometry

2.1 CAD Research

The geometry of a car suspension system is quite complicated and requires significant detail to model. To get an accurate representation of a car suspension system, a CAD file website source was used; GrabCad.com. During our research, we quickly found that there are no available car suspension CAD files that are in Solidworks file format. There were a few options, but they did not accurately represent a full car suspension system. Instead, we decided to bring the scale of the project down a step. We decided to focus our analysis on the shock absorber. A shock absorber CAD file was downloaded and will be used for further analysis. Drawings are shown below.

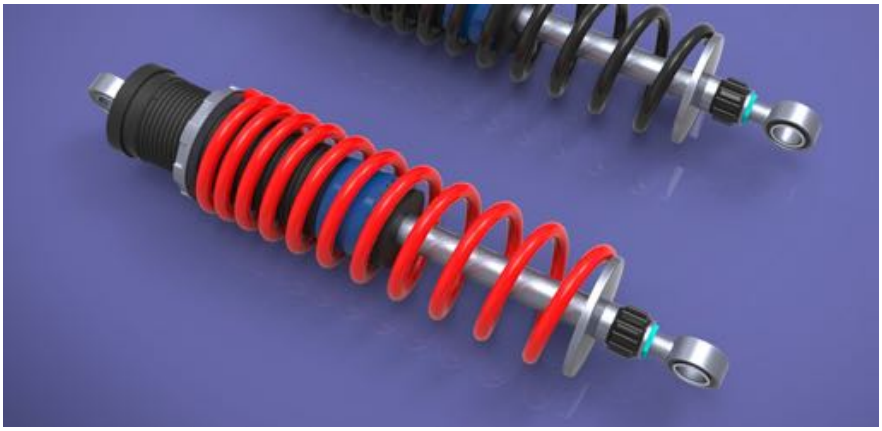

Figure 2.1: Isometric View of Shock Absorber

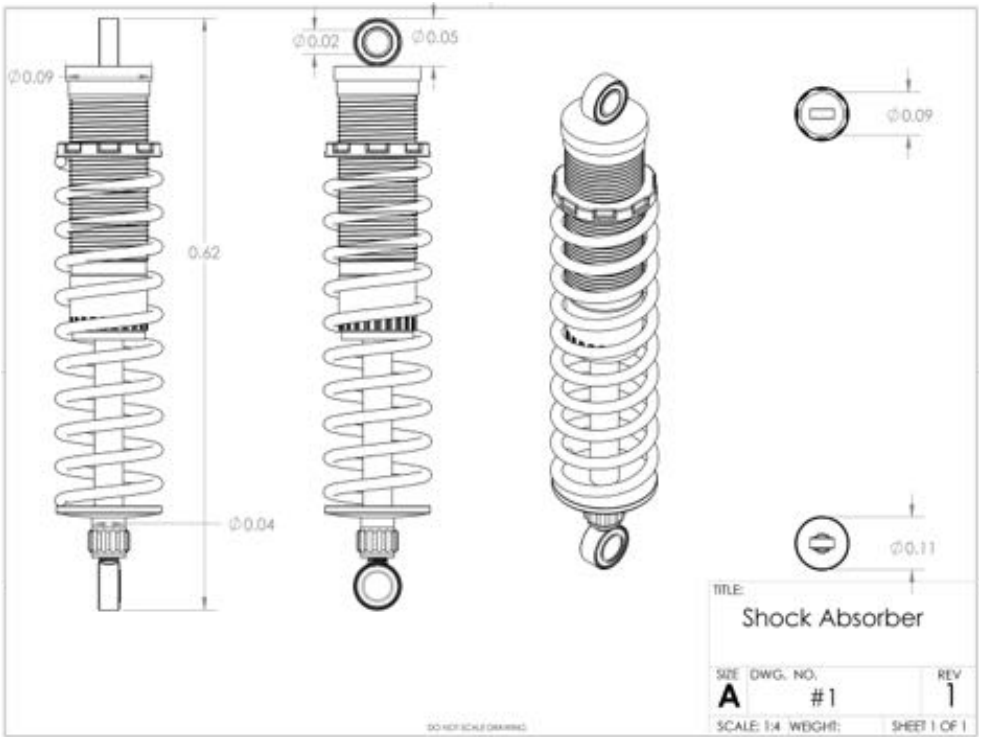

Figure 2.2: Dimensioned Drawing of Shock Absorber - units in m

2.2 Model Properties

Material Properties:

Table 2.1: Material properties used in modeling

Materials	**Modulusof Elasticity (GPa)**	**Yield Stress 0.2% offset (GPa)**	**Poisson's Ratio**	**Density ($Kg/m\text{^}3$)**
1040 Steel	207	372	0.28	7845
Chrome Vanadium	203.4	407	0.28	7860
6061 T-6 Aluminum	71.7	276	0.32	2800

The bushings at the top and bottom of the damper assembly are made of 1040 steel.
The spring is made of chrome vanadium. This is a common spring material.
The body, including the damper shaft is made of 6061 T-6 aluminum.

Constitutive laws:

$$\varepsilon_x = \frac{du}{dx}$$

$$\sigma_x = E\varepsilon_x$$

Spring: F = k*x

Damper: F = c*v

Loading Conditions:

Mass of average sedan = 1500 kg

The loads on the shock absorber result from the weight of the car and the base displacement transmitted from the road. For simplicity, the loading conditions were changed to displacement controlled rather than force controlled, with the displacement taking the form of a sinusoid.

Section 3: Development of Finite Element Meshes

In this section, we lay out a detailed explanation of how the shock absorber assembly parts were meshed. Element mesh type, pictures of the mesh, and material properties are explained within each subsection. Our team started with initial meshes which were then refined, and detailed views of the meshes are available in the appendix.

3.1 - Overall Mesh Refinement

The initial geometry of the assembly was directly imported without making any changes to it. The initial resulting mesh was not of good quality, as can be seen below in Figure 3.1.1. If analysis were to continue with this mesh, we would run into convergence issues and long computational times because of the hundreds of thousands of elements. The geometry is simplified by removing unnecessary fillets, edges, and threads from the exterior of the part. Eliminating the threads made the most significant difference, and this reduction is still accurate because the threads were not structural, merely a tool used for actual mechanics to adjust the spring pre-load. The entire assembly uses tetrahedral meshes. The following sections outline each part with a refined mesh.

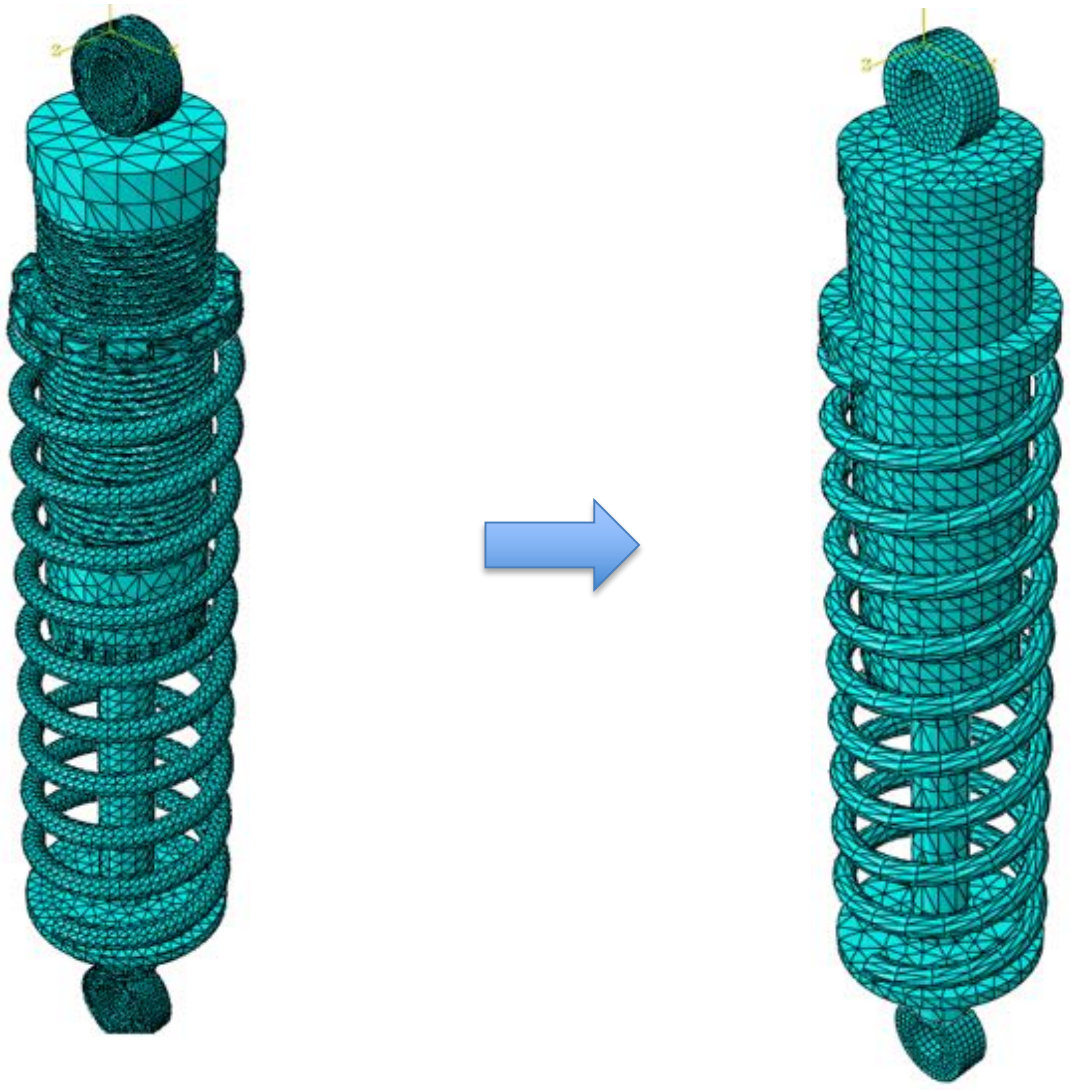

3.2 - Coil Spring Mesh

The coil spring was meshed using tetrahedral elements created through Abaqus's automatic meshing algorithm. In the initial model, a global seed size of 5 was assigned. However, during revision it was determined that a global seed size of 18 was sufficient to accurately represent the spring's geometry. Figure 3.2.1 shows the initial mesh, while Figure 3.2.2 shows the revised mesh. The spring was assigned the properties of chrome vanadium given in section 2, and additional views of the new and revised meshes are available in the appendix.

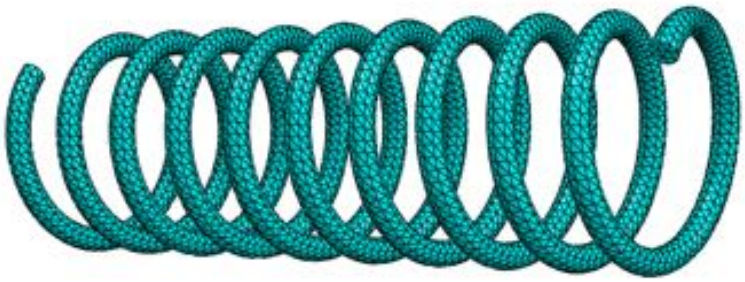

Figure 3.2.1: Initial Coil Spring Mesh

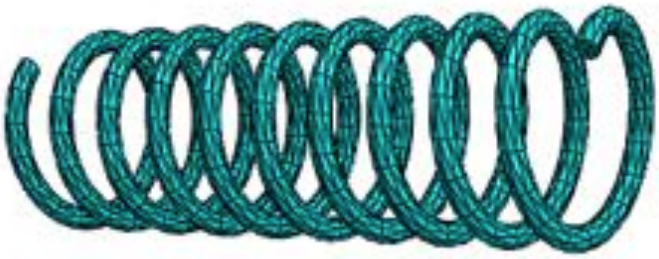

Figure 3.2.2: Final Coil Spring Mesh

3.3 – Hydraulic Piston Mesh Development

The mesh for this part was created by initially assigning global seeds of 8. The next step is selecting the type of mesh for the part; in this part of the shock absorber, tetrahedral meshing was designated due to the complexity of the geometry. The final step was meshing the part as shown in Figures 3.3.1. When the geometry and meshes were refined, the fillets in the base of the piston were removed and the simpler geometry was well represented with a global seed of 20.

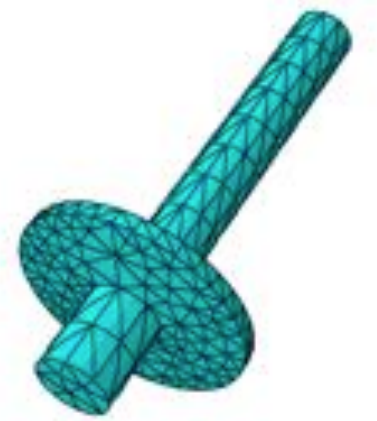

Figure 3.3.1: Initial Hydraulic Piston

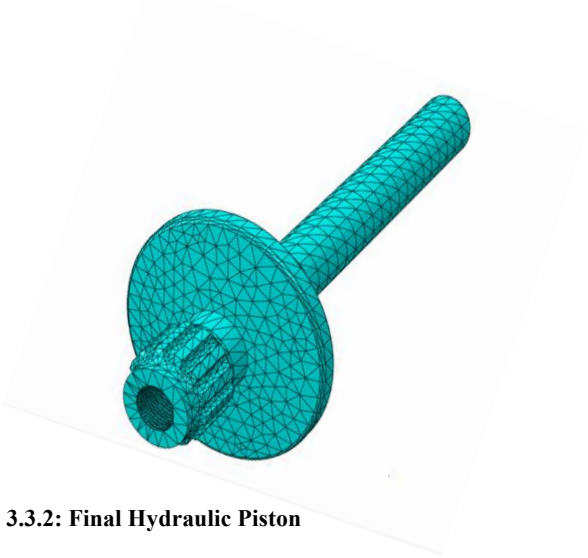

Figure 3.3.2: Final Hydraulic Piston

The oil piston's material properties assigned in abaqus are those of 1060 T6 Aluminum, and can be found in section 2 of this report.

3.5 - Top Shock Absorber Support Mesh

For this initial part, the global seed was 3. Once the global seeds were assigned, automatic tetrahedral meshing was used to create the part, shown in Figure 3.5.1. Upon revision, the support bushing was simplified into a less detailed cylinder with a global seed of 4, shown in Figure 3.5.2. The material used for this part is carbon steel.

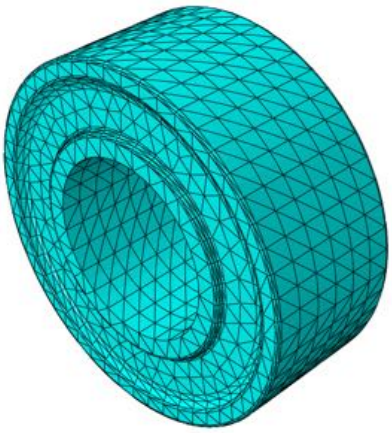

Figure 3.5.1: Original Top Support

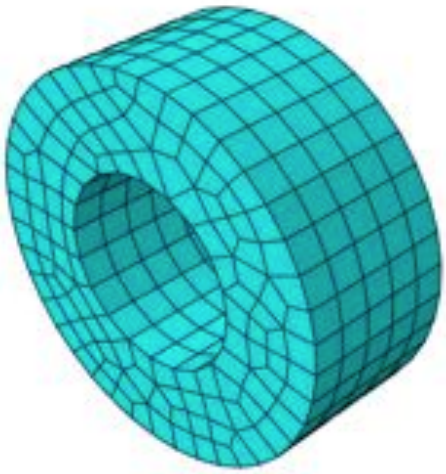

Figure 3.5.2: Revised Top Support

3.6 – Bottom Shock Absorber Support

For the third component of the shock absorber the initial global seed size was 3. Once the global seeds were assigned, the meshing process continued to automatic tetrahedral meshing of the part, shown in Figure 3.6.1. Upon revision, many details of the geometry were reduced; the threads were removed and the edges on the bottom cylinder were smoothed. Once the geometry was simplified, the global seed size required to mesh the part well became 8, and that mesh is shown in Figure 3.6.2.

The material used for this part is carbon steel.

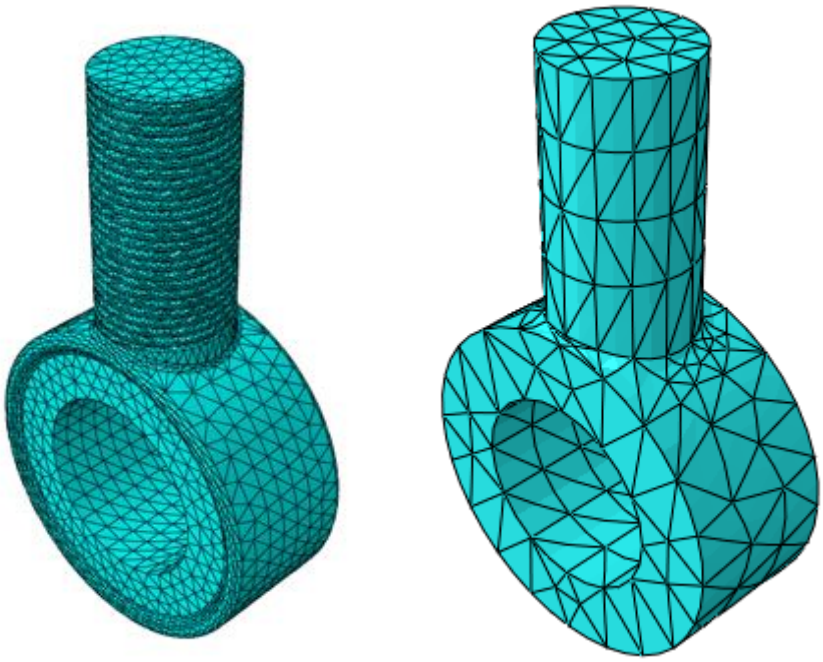

3.7 – Pressure Tube

The pressure tube shown in Figure 3.7.1 initially had one of the most complex geometries of the shock absorber assembly. The mesh quality in this part was significant because it needed to accurately represent small features like the threads. The part was meshed automatically with an approximate global seed of 10. The elements chosen were tetrahedral with a quadratic geometric order because they are able to accurately represent the many curved details of this part. When the part was simplified the features like the threads and fillets were removed. The global seed size was kept at 10, but the mesh became more uniform, as seen in Figure 3.7.2.

Figure 3.7.1: Initial Pressure Tube

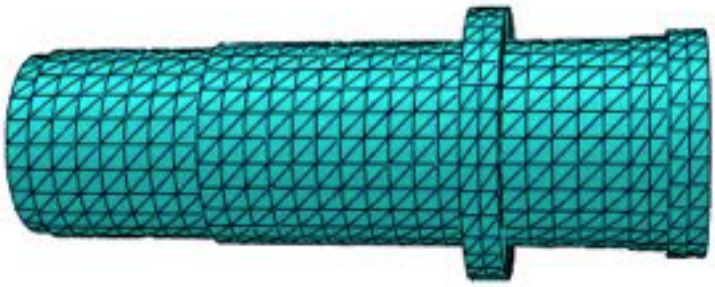

The pressure tube is made of 1061 T6 Aluminum.

Section 4: Development and Description of the Model Assembly and Boundary Conditions

To implement the model assembly and output result, the following had to be defined: material properties, interactions, step, and boundary conditions. The initial modelling efforts are described below; the final model development is detailed in section 6.

Material Properties:

In the initial attempts to run the model, carbon steel material was used throughout the whole part. This was to simplify the model for the team's objectives. The density of the material was selected to be 7850 kg/m^3, the elastic modulus is 190 GPa, and the poisson's ration is 0.27.

Units:
The length scale of our model is in mm. The table below is used to propagate the appropriate units when assigning material properties.

MASS	LENGTH	TIME	FORCE	STRESS	ENERGY	DENSITY	YOUNG's	35MPH 56.33KMPH	GRAVITY
kg	mm	s	mN	1.0e+03 Pa		7.83e-06	2.07e+08		9.806e+03

Step:
Dynamic, Implicit analysis was chosen specifically so that general contact could be used instead of assigning specific contact surfaces and interactions. The geometry of the problem is too complex to accurately assign contact surfaces, especially because as the parts move the contacting surfaces change. General contact applies the same properties to any surfaces that touch. The preliminary results used a total step time is 1 second. The final model uses a total step time of 0.25 seconds to simulate real conditions.

Interactions:
General contact interaction was applied during the initial step of the simulation to simplify the process of creating contact surfaces. We had to make sure to assign the interaction during the initial step, otherwise general contact was not an option. The coefficient of friction, 0.3, applied to this interaction was determined from literature.
The model used the following interactions inputs:
General contact –
(1) Interaction property: Contact: Mechanical: tangential: Penalty: frictional (0.3)

Boundary Conditions:
The boundary conditions applied to the model were critical to creating a realistic load pattern. Because the goal of a shock absorber is to minimize the motion of the car body, the top bracket was constrained to be immobile. The rest of the shock absorber was constrained to allow motion only in the vertical (y) direction. Finally, the load was applied; a traction force of 25,000 N was applied to the bottom bracket in the vertical direction, and it was directed to gradually increase over the duration of step 1 because loads cannot be applied fully instantaneously.

Refining the Mesh:
The mesh elements were created initially as tetrahedral elements sized depending on the complexity of each part's geometry. These meshes were sufficient to get good results from the model without any convergence or other errors.

Preliminary Results:
The first running version of this model showed the stresses in the shock absorber as the load was gradually applied over a time period of one second. This loading pattern reflects the type of loads that could be imparted by bumps in a road surface: gradually applied over a fast period of time. The figures below show the stresses on the shock absorber at various time intervals within the loading period.

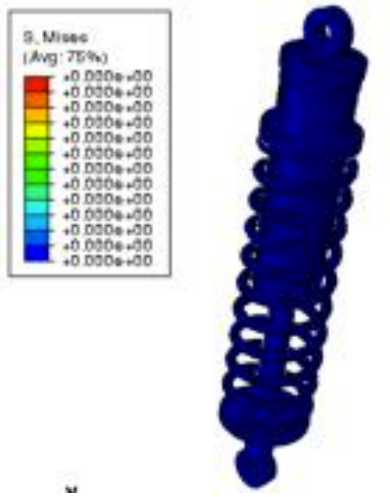

Figure 2: Time = 0

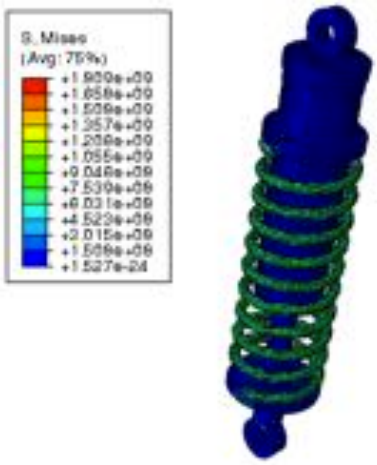

Figure 3: Time = 0.1s

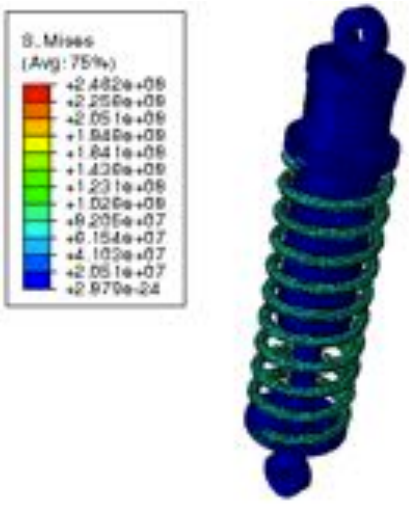

Figure 4: Time = 0.31s

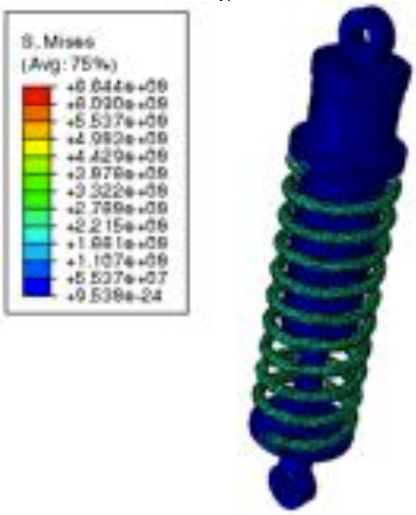

Figure 5: Time = 1s

The maximum stress indicated during this loading occurs at Time = 1s, when the full load is applied to the system. The highest visible stress value is approximately 4.5 GPa and is located along the inner spring surface. The implications of these results are that the spring, especially under cyclic loads, would be at the greatest risk of yield and/or fatigue failure in the shock absorber assembly. Also, under this assigned load the carbon steel of the spring would have yielded because its yield stress is approximately 370 MPa. However, this load was selected for the preliminary model in order to more easily visualize results, not for accuracy; a more accurate load on the shock absorber would be closer to 5000 N from the weight of the car and then an additional force resulting from the car's displacement from the road surface. Future iterations of the model will focus on improving accuracy.

Section 5: Development and Description of Model Interactions

In this model the parts sliding against each other require friction interactions between the surfaces. Implicit Dynamic step was selected in order to analyze the stresses in the parts as they move, and because general contact was an option for surface interactions. In this model all of the friction interactions were estimated to be the same between each part. This makes general contact a reasonable interaction choice because it assigns the same properties to each surface, with the added benefit that it does not require the assignment of master-slave or other more complex relationships.

Section 6: Analysis of Finite Element Model

Describe how you ran your simulation, e.g. step type, static, dynamic, etc. how many procs. How long did run.

The final version of this simulation used the general procedure performed in the initial model development, but with several updates once more realistic material properties and loading patterns were determined. This section will describe the final model as well as how the analysis was performed.

Material Properties:

The final model used the material properties identified in section 2. The bushings and spring were given the same material properties, those of chromium vanadium, because the properties of the chromium and 1040 steel are very similar and using fewer materials simplified the contact specifications. The pressure tube and piston were assigned the properties of 1061 Aluminum.

Units:

The length scale of our model is in mm. The table below is used to propagate the appropriate units when assigning material properties.

MASS	LENGTH	TIME	FORCE	STRESS	ENERGY	DENSITY	YOUNG's	35MPH 56.33KMPH	GRAVITY
kg	mm	s	mN	1.0e+03 Pa		7.83e-06	2.07e+08		9.806e+03

Step:

Static, General analysis was chosen for the final model. This is different than the initial modelling attempts because it was determined that surface-to-surface interactions were needed. The step lasts a duration of 0.25 seconds with nonlinear geometry turned on.

Interactions:

General contact and surface-surface interactions were created in the initial step of the model. We had to make sure to assign the interactions during the initial step, otherwise general contact was not an option. The general contact interactions were given a coefficient of friction of 0.3 with tangential penalty behavior. The surface-surface interactions were specified for the contact between the piston and the pressure tube, and given a coefficient of 0.2.

Boundary Conditions:

The boundary conditions applied to the final model were the same as those applied to the initial model. Because the goal of a shock absorber is to minimize the motion of the car body, the top bracket was constrained to be immobile using an encastre condition. The rest of the shock absorber was constrained to allow motion only in the vertical (y) direction. Finally, the load was applied; the final model had a cyclical base displacement applied to the bottom bushing. The magnitude of the displacement is 120mm, larger than a typical road disturbance but intended to show trends in the behavior. The frequency of the cyclic displacement is such that the 0.25sec step encompasses one full cycle.

Refining the Mesh:
Using the simplified geometry specified above, a tetrahedral mesh was automatically generated. The mesh automatically seeded the parts to that the smaller features were more detailed. Attempts to run the model using the automatic mesh were successful, so it was concluded that the automatic mesh was sufficient.

Computational Requirements:
Between all of the parts, the simplified geometry of this model had about 18,000 elements to solve. Solving this model took about one hour using four processing nodes.

Results:
The first running version of this model showed the stresses in the shock absorber as a load was gradually applied over a time period of one second. The final version shows the stresses resulting from a cyclic load over a time period of 0.25 seconds. This loading pattern reflects the type of loads that could be imparted by bumps in a road surface: gradually applied over a fast period of time. The progression of stress distributions throughout the cycle of loading is shown in the figure:

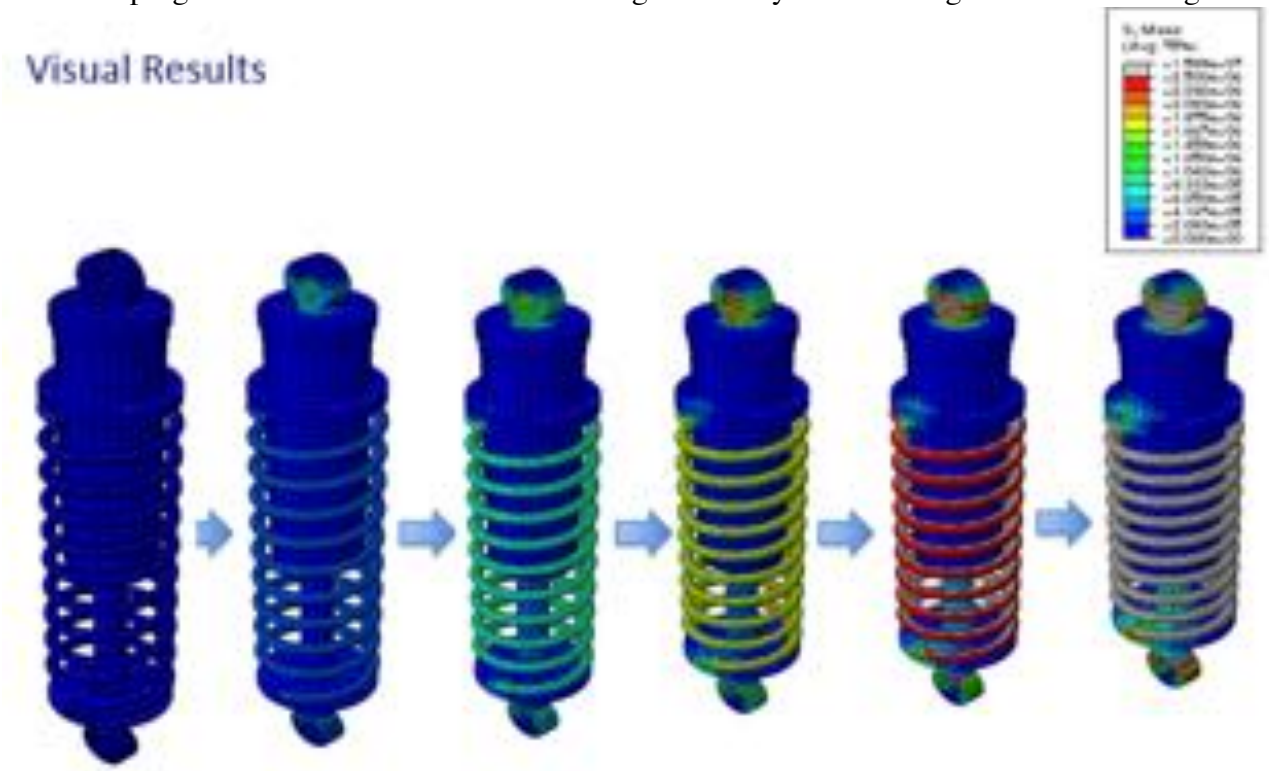

The maximum stress indicated during this loading occurs when the maximum displacement is applied. The maximum stress under this loading has a value of approximately 16 GPa and is located along the inner spring surface. The implications of these results are that the spring, would be at the greatest risk of yield and/or fatigue failure in the shock absorber assembly. Under this assigned load the chrome vanadium of the spring would have yielded because its yield stress is approximately 400 MPa. However, though the cyclic load is more accurate than the ramp load applied in the preliminary model, the magnitude of this load was still selected to more easily visualize results, not for accuracy. A more accurate displacement magnitude for the shock absorber would be closer to 50mm, so the stresses in the spring in this model are likely at least twice what their true values would be.

Section 7: Summary of Major Findings

The most significant results from this modelling project are the locations of maximum stress in the shock absorber. From the visual results, the maximum stress loads occur on the interior surface of the spring and on the neck of the bushing. Figure 7.1 below shows the range of stresses in a segment of the spring, with different locations demonstrating significantly different loads.

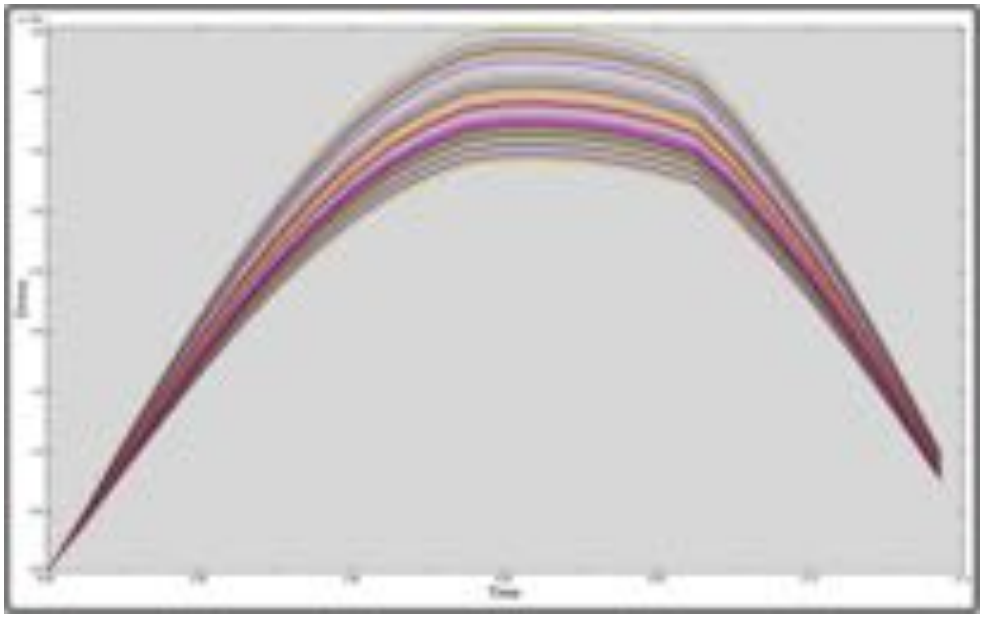

Section 8: Works Cited

I suggest to use Mendeley for citing references. It is free. Get it from : https://www.mendeley.com/

Material Properties:

- *Metals and Alloys - Densities*. N.p., n.d. Web. 05 Feb. 2016.
- *Wikipedia*. Wikimedia Foundation, n.d. Web. 05 Feb. 2016.
- "Iso-Grade Oil." *Engineering Toolbox.* N.d. Web. 04 Feb. 2016. http://www.engineeringtoolbox.com/iso-grade-oil-d_1207.html

Appendix 1: Mesh Development Images

Coil Spring Initial:

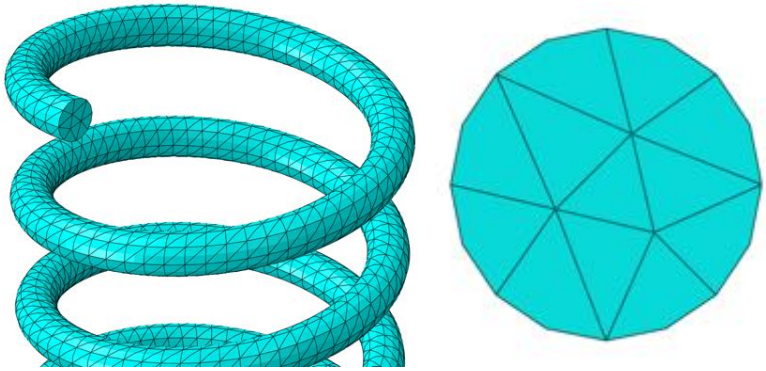

Revised:

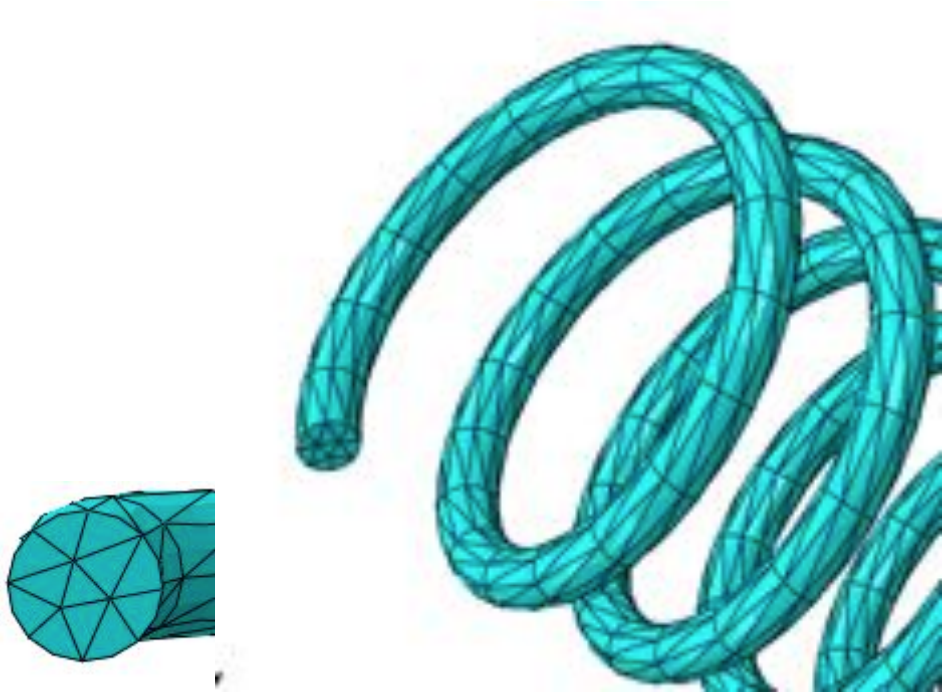

Hydraulic Piston Initial:

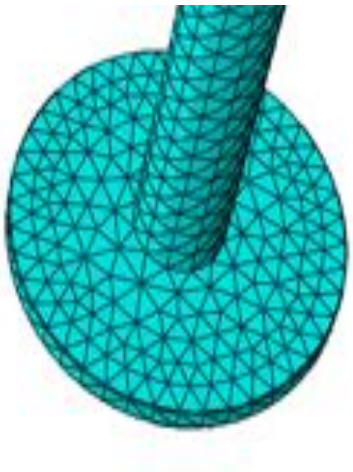

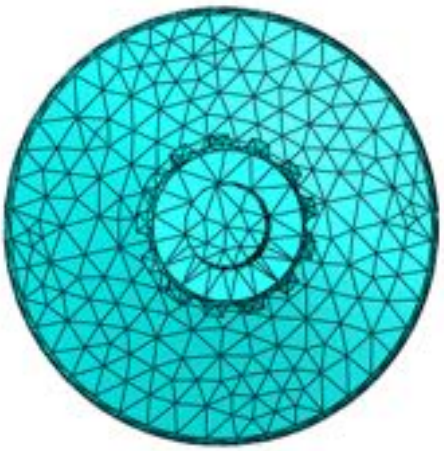

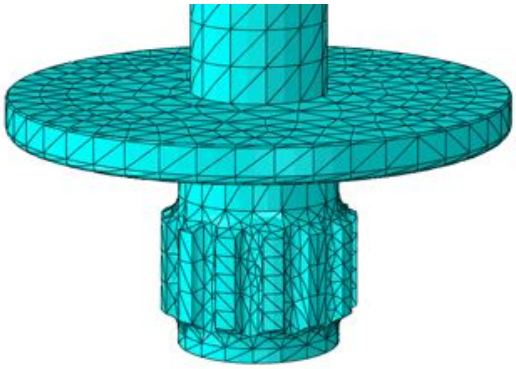

Revised:

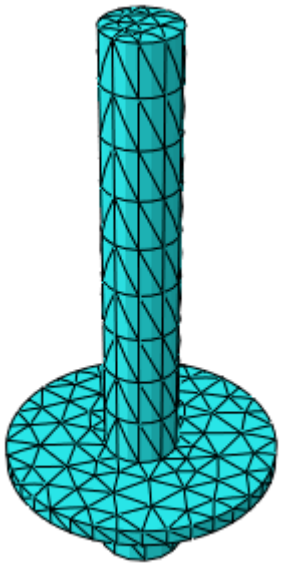

Top Support Bushing Initial:

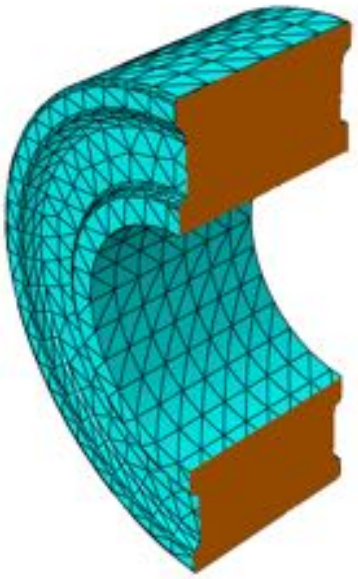

Bottom Support Bushing

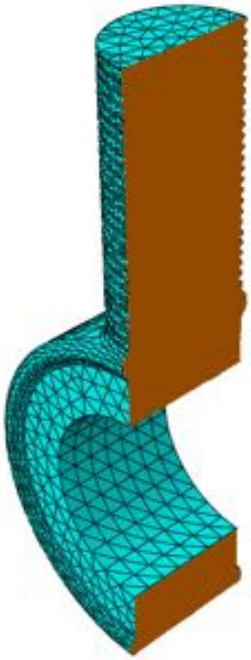

Pressure Tube Initial:

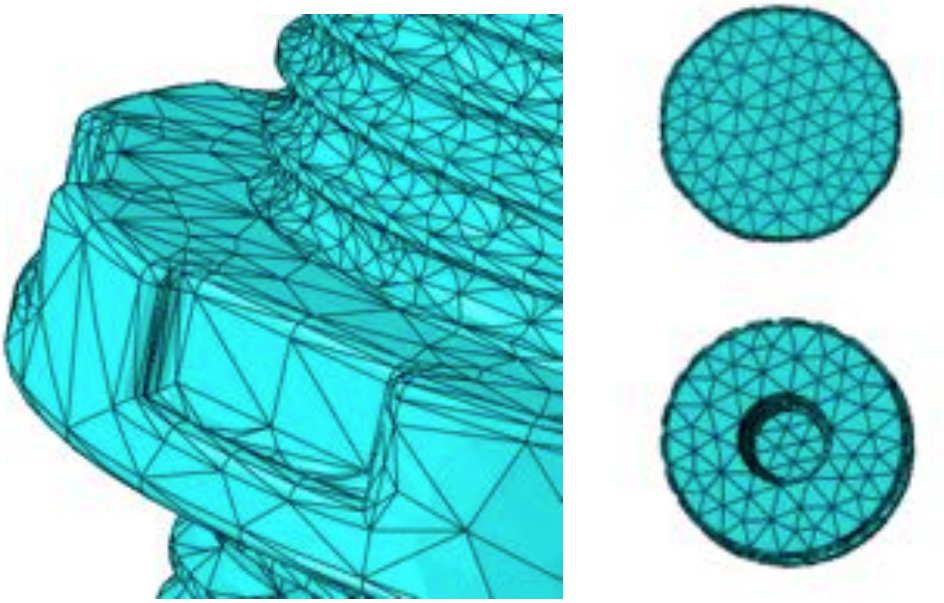

Revised: